Calcium/Calmodulin-dependent Protein Kinase II (CaMKII) Inhibition Induces Neurotoxicity via Dysregulation of Glutamate/Calcium Signaling and Hyperexcitability*[S]

Nicole M. Ashpole[‡], Weihua Song[‡], Tatiana Brustovetsky[§], Eric A. Engleman[¶], Nickolay Brustovetsky[‡§],
Theodore R. Cummins[‡§], and Andy Hudmon[¶1]

*From the [‡]Stark Neuroscience Research Institute, Departments of [§]Pharmacology and Toxicology, [¶]Psychiatry, and [||]Biochemistry
and Molecular Biology, Indiana University of School of Medicine, Indianapolis, Indiana 46202*

Background: Loss of CaMKII correlates with neuronal death following stroke and traumatic brain injury, yet whether this contributes to neurotoxicity is not known.
Results: CaMKII inhibition induces dysregulation of neuronal calcium and glutamate homeostasis, increases excitability, and induces apoptosis.
Conclusion: CaMKII inhibition plays a causal role in neurotoxicity.
Significance: Understanding the impact of CaMKII inactivation is crucial for developing therapeutics for ischemia/traumatic brain injury.

Aberrant glutamate and calcium signalings are neurotoxic to specific neuronal populations. Calcium/calmodulin-dependent kinase II (CaMKII), a multifunctional serine/threonine protein kinase in neurons, is believed to regulate neurotransmission and synaptic plasticity in response to calcium signaling produced by neuronal activity. Importantly, several CaMKII substrates control neuronal structure, excitability, and plasticity. Here, we demonstrate that CaMKII inhibition for >4 h using small molecule and peptide inhibitors induces apoptosis in cultured cortical neurons. The neuronal death produced by prolonged CaMKII inhibition is associated with an increase in TUNEL staining and caspase-3 cleavage and is blocked with the translation inhibitor cycloheximide. Thus, this neurotoxicity is consistent with apoptotic mechanisms, a conclusion that is further supported by dysregulated calcium signaling with CaMKII inhibition. CaMKII inhibitory peptides also enhance the number of action potentials generated by a ramp depolarization, suggesting increased neuronal excitability with a loss of CaMKII activity. Extracellular glutamate concentrations are augmented with prolonged inhibition of CaMKII. Enzymatic buffering of extracellular glutamate and antagonism of the NMDA subtype of glutamate receptors prevent the calcium dysregulation and neurotoxicity associated with prolonged CaMKII inhibition. However, in the absence of CaMKII inhibition, elevated glutamate levels do not induce neurotoxicity, suggesting that a combination of CaMKII inhibition and elevated extracellular glutamate levels results in neuronal death. In sum, the loss of CaMKII

observed with multiple pathological states in the central nervous system, including epilepsy, brain trauma, and ischemia, likely exacerbates programmed cell death by sensitizing vulnerable neuronal populations to excitotoxic glutamate signaling and inducing an excitotoxic insult itself.

Precisely regulated calcium signaling is essential for normal neuronal growth and survival. Although slight fluctuations in intracellular calcium concentration are tolerated by neurons and necessary for a variety of physiological processes, dysregulation of intracellular calcium leads to neuronal death. Intracellular calcium overload can lead to mitochondrial depolarization and the overactivation of the downstream signaling pathways regulated by calcium. One important signaling pathway that is activated by calcium signaling is calcium/calmodulin (CaM)-dependent protein kinase II (CaMKII).[2] Following activation with calcium-bound calmodulin, CaMKII targets to and phosphorylates a number of substrates in neurons, including voltage- and ligand-gated calcium channels, cAMP-response element-binding protein, ERK, and voltage-gated sodium channels (1–3).

Fluctuations in CaMKII activity have been associated with neuronal disease states that exhibit excitotoxic calcium dysregulation, such as stroke, epilepsy, and traumatic brain injury (4–11). Immediately following the onset of excitotoxic stimulation, CaMKII is activated (5, 9), and inhibition of CaMKII prior to excitotoxic insult prevents neuronal damage both *in vitro* and *in vivo* (12–17). However, αCaMKII knock-out animals paradoxically exhibit a significant increase in neuronal damage following stroke compared with wild-type littermates

[2] The abbreviations used are: CaM, calmodulin; CAMKII, calcium/calmodulin-dependent kinase II; ANOVA, analysis of variance; DIV, days *in vitro*; GPT, glutamate pyruvate transaminase; Fam, 6-carboxyfluorescein; ANOVA, analysis of variance; NMDA-R, NMDA receptor; AIP, auto-inhibitory peptide.

(18). Moreover, we recently showed that prolonged pharmacological inhibition of CaMKII actually exacerbated excitotoxicity following a submaximal glutamate challenge (12). Thus, although an acute loss of CaMKII may protect neurons from excitotoxic insult, a prolonged loss of CaMKII activity sensitizes neurons to glutamate toxicity, an observation we hypothesize contributes to programmed cell death in the penumbral region associated with ischemia and brain trauma. In support of this hypothesis, a loss of CaMKII activity has been shown to be spatially correlated with the extent of neuronal damage following focal ischemia (8). The region immediately surrounding the infarct not only displays the greatest damage but also the greatest loss in CaMKII activity (8). However, the ischemic environment is associated with complex biochemical changes that are associated with aberrant glutamate signaling, including enhanced reactive oxygen species activity, acidosis, and a decrease in energy availability. Thus, we chose to investigate neuronal survival, calcium signaling, and excitability following a loss of CaMKII activity induced by a broad spectrum of CaMKII inhibitors in the absence of an exogenous glutamate challenge. Our data support a model whereby prolonged inhibition of CaMKII produces apoptosis in cortical neurons by a feed-forward process associated with neuronal hyperexcitability and dysregulated calcium and glutamate signaling.

EXPERIMENTAL PROCEDURES

Materials—Unconjugated tat (YGRKKRRQRR), CN21 (KRPPKLGQIGRSKRVVIEDDR), CN21Ala (KAPAKAAQAAA-SKRVVIEDDR), CN21C (GQIGRSKRVVIEDDRIDDVLK), tat-AIP (YGRKKRRQRR-KKKLRRQEAFDAL), tat-CN21, tat-CN21Ala, as well as Fam-labeled versions of these peptides were synthesized and HPLC-purified by Biopeptide Co., Inc. San Diego. Myristoylated AIP (64929) was purchased from Anaspec, Fremont, CA. KN-93 (422708) and KN-92 (422709) were purchased from Calbiochem. STO-609 (1551) was purchased from Tocris Bioscience, Ellisville, MO. MK-801 (M107), nifedipine (N7634), nimodipine (N149), tetrodotoxin (T8024), ω-conotoxin (C9915), ifenprodil (I2892), and memantine (M9292) were purchased from Sigma.

Neuronal Cultures—Cortical neurons were harvested from E18 to E19 Sprague-Dawley rat pups according to approved IACUC guidelines as described previously (12). Primary hippocampal neurons were prepared from postnatal day 1 Sprague-Dawley rat pups as described previously (19, 20). For most experiments, cortical neurons were seeded at a density of 2.5 million cells/ml and seeded on poly-D-lysine (50 μg/ml)-coated 15-mm coverslips (German glass Number 0) or 60-mm dishes. For experiments looking at neuronal viability at different stages of culture development, neurons were seeded at 1.25 million cells/ml. Cultures were treated with 5-fluor-2'-deoxyuridine (15 mg/ml) (Sigma, F0503) and uridine (35 mg/ml) (Sigma, U3750) to kill mitotically active cells on days 2–4. Co-cultures of neurons and astrocytes were not treated with these mitotic inhibitors.

Cell Death Assay—Following treatment, the coverslips were washed in PBS and stained using Live/Dead Cytotoxicity/Viability kit (Molecular Probes, Eugene, OR) as described previously (12). Each coverslip is imaged in three different fields using a Texas Red filter to detect cytotoxic cells and a FITC filter to detect viable cells on a Nikon Ti-E inverted microscope ($\times$100 magnification). Cells were quantified using the automated counting software Nikon Elements 3.0 as described previously (12). Total cell number was determined by addition of cytotoxic and viable cells. Complete media exchanges and washing conditions routinely induced cytotoxicity in about 5–10% of cultured neurons.

Immunocytochemistry of Neuronal Cultures—Neurons (8–9 DIV) treated with CaMKII inhibitors were fixed in 4% paraformaldehyde (0.1 M phosphate buffer, pH 7.4) for 10 min and washed in phosphate-buffered saline (PBS) three times. For labeling, cells were permeabilized in 0.5% Triton X-100 in PBS for 10 min at room temperature, washed in PBS three times, blocked for 1 h in 2% BSA fraction V, 20% normal goat serum, 0.1% Triton X-100 in PBS at room temperature, and washed an additional three times in PBS. Cells were then incubated in primary polyclonal cleaved caspase 3 antibody (1:500, Cell Signaling (9661), Beverly, MA) for 2 h at room temperature. After three washes, secondary antibodies (anti-rabbit Alexa 594, 1:5000 (Molecular Probes, Eugene, OR)) were applied for 1 h at room temperature. Coverslips were washed in PBS three times and were subsequently mounted in Prolong Gold Antifade with DAPI mounting media (Molecular Probes), and cells were imaged using a Zeiss Axio ObserverZ1 and processed with Axiovision 4.

CaMKII Activity Assay—Neuronal cultures were lysed in lysis buffer containing 50 mM HEPES, pH 7.4, 4 mM EGTA, 10 mM EDTA, 15 mM $Na_4P_2O_7 \cdot 10H_2O$, 100 mM β-glycerophosphate, 25 mM NaF, 1% Triton X-100, and protease inhibitor mixture (Calbiochem, 539137) as described previously (21), sonicated, and incubated with 50 mM HEPES, pH 7.4, 100 mM NaCl, 10 mM $MgCl_2$, 100 μM ATP, 2 mM $CaCl_2$, 5 μM CaM, 50 μM AC2 (KKALRRQETVDAL), and [γ-^{32}P]ATP (3 μCi per reaction) for 3 min at 30 °C. The linear range of the reaction extended from 30 s to 4 min. Protein levels were assessed, and activity was normalized to total protein using DC protein assay kit (Bio-Rad).

Calcium Imaging—Hippocampal neurons 10–12 DIV were loaded with 2.6 μM Fura-2FF-AM (Invitrogen) and 1.7 μM Rhodamine 123 and subsequently imaged as described previously (20, 22). During imaging, the neurons were maintained in a bath solution containing 10 mM HEPES, pH 7.4, 139 mM NaCl, 3 mM KCl, 0.8 mM $MgCl_2$, 1.8 mM $CaCl_2$, 5 mM glucose, and 65 mM sucrose. For Fluo-4 experiments, cortical neurons were incubated with 5 μM Fluo-4-AM (Invitrogen) diluted in rat physiological saline (138 mM NaCl, 2.7 mM KCl, 1.8 mM $CaCl_2$, 1.06 mM $MgCl_2$, 12.4 mM HEPES, pH 7.4, 5.6 mM glucose; final pH adjusted to 7.3) for 30 min at 37 °C. Following incubation, cells were washed with rat physiological saline three times for 5 min each. A Nikon Ti-E inverted microscope with a FITC filter was employed to monitor Fluo-4 levels once every 30 s. Base line was monitored for 5 min. In all experiments with CaMKII inhibitor application, the inhibitor was added 10 min after start of imaging, and some experiments called for the addition of other inhibitors as indicated. For these, the drugs were applied at the 5-min mark to identify whether the drug itself had an impact on calcium levels prior to CaMKII inhibitor application

at minute 10. Analysis was performed using Nikon Elements version 3.0 in which Fluo-4 levels were measured in ~20 cells per field and three fields per coverslip. Neurons were identified at the start of the experiment with a 20 mM KCl depolarization with a subsequent wash. The fluorescent intensity of each cell was normalized to time 0, as the drug was applied.

Electrophysiology—Action potential studies were carried out using the whole cell patch clamp technique under the current clamp mode. Whole cell voltages were recorded with HEKA software (HEKA Electronik). The neuronal growth media on the cortical neurons (8–10 DIV) were gradually replaced by the extracellular recording solution before the patch clamp recording. The extracellular solution consisted of rat physiological saline (as described above). The intracellular solution contains 140 mM potassium gluconate, 2 mM KCl, 3 mM $MgCl_2$, 10 mM HEPES, 5 mM phosphocreatine, 2 mM potassium ATP, 0.2 mM sodium GTP, and final pH adjusted to 7.4. Pipette resistance was 2–4 megohms when filled with the internal solution. Data were acquired and analyzed using the Pulsefit software following previously established protocols (23, 24). Cortical neurons were held at their resting potentials by injection of steady current throughout the experiment. To determine the current threshold for action potential initiation, neurons were injected with a series of depolarizing currents with variable amplitudes for 200 ms. The sampling frequency was 10 kHz. Following identification of the current threshold for action potential generation, neurons were injected with a 1-s depolarizing ramp current that subsequently elicited one to two action potentials. Neurons that maintain initial resting membrane potentials more negative than −50 mV after whole cell configuration and had less than three action potentials at the starting point were included in this study. We compared the change in the number of action potentials obtained 10 min after establishing the whole cell configuration to the number obtained at the initial starting time point when the peptide had not diffused into the intracellular environment. The current clamp studies were performed at room temperature (~21 °C).

Glutamate Measurements—Glutamate concentrations in the neuronal media were assessed using Amplex Red glutamic acid/glutamate oxidase assay per manufacturer's protocol (Invitrogen). The glutamate detection assay standard curve was linear from 180 nM to >6 μM glutamate. For high performance liquid chromatography quantification, glutamate was measured by HPLC separation and electrochemical detection of an *O*-phthalaldehyde-mercaptoethanol derivative using modifications of the method of Donzanti and Yamamoto (25). See supplemental Fig. 4 for more detail.

Data Analysis—Electrophysiology data are presented as the mean ± S.E. Statistical significance between groups was determined using one-way ANOVA with a post hoc Bonferroni's test. One-way ANOVA with a subsequent Dunnett's test was conducted to compare differences between the means of each group in all *in situ* cell death assays, *in vitro* catalytic assays, and calcium imaging experiments. Student's *t* test was also used when appropriate. Statistical significance was accepted at $p <$ 0.05. Analysis was performed using SigmaPlot 11 software.

RESULTS

Neurotoxicity with CaMKII Inhibition—To test the hypothesis that CaMKII inhibition induces neuronal death, we subjected cortical neurons (8 DIV) to acute (1 h) and prolonged (24 h) pharmacological inhibition of CaMKII using multiple inhibitors. Peptides derived from the endogenous inhibitor of CaMKII, termed CN21, and the autoinhibitory domain of CaMKII itself (AIP) were used because of their high specificity to inhibit CaMKII (26–28). As described previously (12, 13, 27), conjugation of peptide inhibitors to the cell-penetrant motif, tat, affords the ability to examine the effects of CaMKII inhibition with cell-penetrating peptides in both cultures and *in vivo*. In addition to the peptide inhibitors, we also utilized the allosteric CaMKII inhibitor KN-93 (12, 27–29). We applied 10 μM tat-CN21, tat-AIP, and 1 μM KN-93 to cortical neuronal cultures for 1 or 24 h and subsequently examined viability/cytotoxicity levels 24 h following the start of treatment (12). To compensate for the decreased bioavailability associated with tat-based peptides accumulating in noncytoplasmic compartments (30), the concentrations of the peptide inhibitors used in this study are roughly 100-fold above the *in vitro* IC_{50} for CN21 (77–100 nM) (12, 27). To control for potential off-target effects, we applied KN-92, the inactive control for KN-93, or a peptide control, tat-CN21-Ala (12). For each neuronal death experiment, data were normalized by subtracting average neuronal death observed in control cultures. The control cultures in each experimental group consistently exhibited 5–10% toxicity. Cortical neuron viability was no different from control cultures (DMSO-treated) when CaMKII inhibitors were applied for 1 h (Fig. 1*A*, *gray bars*). In contrast, all three CaMKII inhibitors (KN93, tat-CN21, and tat-AIP) significantly increased neuronal death 12–18% when applied for 24 h (Fig. 1*A*, *black bars*). Compared with control cultures, lower concentrations of tat-CN21 also induced neurotoxicity when applied overnight (1 μM tat-CN21 5.3 ± 2.4%; $p < 0.05$). Importantly, cultures treated with the inactive controls, tat-CN21Ala and KN-92, for 24 h did not exhibit significant changes in neuronal viability (Fig. 1*A*), suggesting that the neurotoxic effects are specific to the application of active small molecules and peptide CaMKII inhibitors. Furthermore, the tat motif itself was not toxic when applied for 24 h (0.533 ± 1.6%; $p > 0.05$). Utilization of a myristoylated AIP peptide inhibitor of CaMKII also induced neurotoxicity (29.6 ± 4.2%; $p < 0.05$). Thus, CaMKII inhibition using both small molecule and peptide inhibitors conjugated to tat and myristoylated cell-penetrating motifs induce neuronal death when applied for 24 h.

Although a significant increase in neurotoxicity was observed within our neuronal cultures when CaMKII was inhibited at 8 DIV, we tested whether the age of the culture affected this neuronal death. Although no differences were observed in neuronal viability between control groups at 8, 14, and 21 DIV, 24 h of inhibition of CaMKII with tat-CN21 significantly enhanced neurotoxicity with respect to time in culture (Fig. 1*B*). Compared with cultures 8 and 14 DIV, cultures exhibited nearly 25% toxicity, and nearly 75% of cells were compromised when CaMKII was inhibited at 21 DIV. The cell death observed with CaMKII inhibition was not limited to highly

FIGURE 2. **Time dependence of neurotoxicity and CaMKII inactivation with CaMKII inhibition.** *A,* neuronal death (mean ± S.E., $n = 7$–12) normalized to control when 10 μM tat-CN21 was applied to neuronal cultures for varying lengths of time. *, $p < 0.05$ compared with control (one-way ANOVA, post hoc Dunnett's test). *B,* kinase activity (mean ± S.D., $n = 3$–4) in neuronal lysates subjected to an *in vitro* CaMKII assay in the presence of calcium/calmodulin after 10 μM tat-CN21 (or tat-CN21Ala) was applied to cortical neurons for varying lengths of time. *, $p < 0.05$ compared with control (one-way ANOVA, post hoc Dunnett's test).
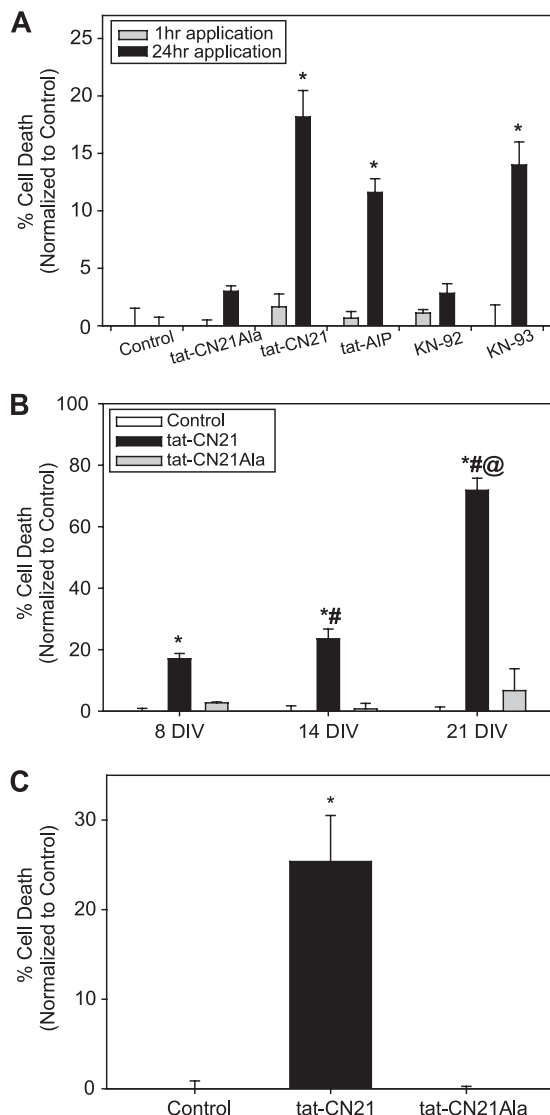
FIGURE 1. **Neurotoxicity with CaMKII inhibition.** *A,* neuronal death (mean ± S.E., $n = 3$–15) normalized to control when CaMKII inhibitors (10 μM peptide inhibitors and 1 μM small molecule inhibitors) were applied to neuronal cultures (8 DIV) for 1 h (*gray bars*) or 24 h (*black bars*). *, $p < 0.05$ compared with control (one-way ANOVA, post hoc Dunnett's test). *B,* neuronal death (mean ± S.E., $n = 4$–17) normalized to control when 10 μM tat-CN21 or tat-CN21Ala was applied to neuronal cultures for 24 h at 8, 14, and 21 DIV. *, $p < 0.05$ compared with control at that time point; #, $p < 0.05$ compared with 8 DIV tat-CN21 treatment (one-way ANOVA, post hoc Dunnett's test). @, $p < 0.05$ for 14 DIV tat-CN21 treatment *versus* 21 DIV tat-CN21 treatment (*t* test). *C,* neuronal death (mean ± S.E., $n = 4$) normalized to control when 10 μM tat-CN21 or tat-CN21Ala was applied to co-cultures for 24 h. *, $p < 0.05$ compared with control (one-way ANOVA, post hoc Dunnett's test).

enriched cortical cultures (>95% MAP2-immunopositive (12)), as a similar level of toxicity was observed in neurons cultured with glia (Fig. 1*C*). In these co-cultures, a monolayer of glial fibrillary acidic protein-positive astrocytes underlying MAP2-positive cortical neurons represents an astrocyte to neuron ratio of 3:2 (supplemental Fig. 1). Thus, the toxicity produced by CaMKII inhibition is enhanced by culture age and observed in both highly pure cultures of cortical neurons as well as cortical neurons cultured with astrocytes.

In Fig. 1*A* we report that CaMKII inhibition for acute (1 h) *versus* prolonged (24 h) periods differentially affects neuronal death. To determine the minimal time for CaMKII inhibition-
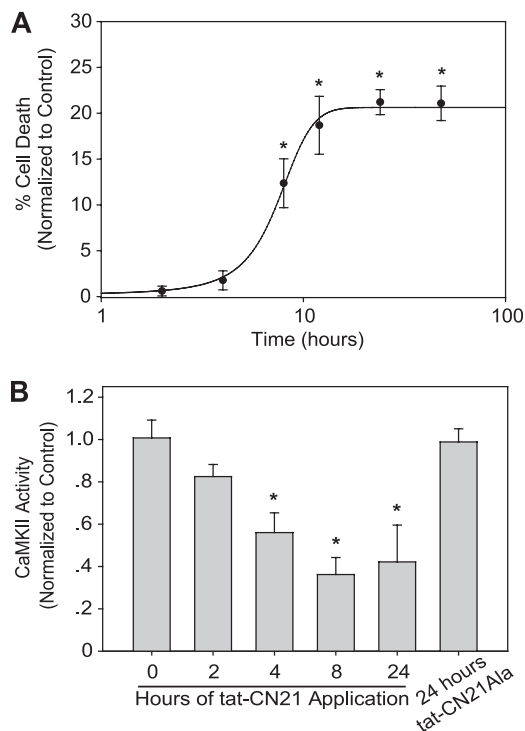
induced cell death, we applied tat-CN21 for various times between 1 and 24 h. In addition, we explored exposure times longer than 24 h to determine whether neurotoxicity was saturated. Once again, a 1-h exposure of neurons to tat-CN21 failed to produce cell death (Fig. 2*A*). CaMKII inhibition for 4 h or less was also not toxic to neurons (Fig. 2*A*). Progressively increasing neuronal death as a function of CaMKII inhibition time was observed up to 12 h. However, longer incubation times (24 or 48 h) did not produce additional neurotoxicity (Fig. 2*A*), suggesting that events occurring within the first 12 h largely determine the neuronal death associated with CaMKII inhibition.

The extent of CaMKII inactivation produced by focal ischemia *in vivo* was previously shown to correlate with the extent of neuronal damage (8). Because we observed a time dependence in the neurotoxicity produced by CaMKII inhibition, we determined if neuronal death in cortical cultures is correlated with functional changes in CaMKII. We observed a time-dependent loss in the activatable pool of CaMKII that correlated with exposure time of the CaMKII inhibitor. Application of tat-CN21 for ≥4 h resulted in a significant decrease in activatable CaMKII compared with vehicle-treated control neurons (Fig. 2*B*). A maximal 50% loss of activity occurred when tat-CN21 was applied for 24 h. Importantly, neurons treated with inactive tat-CN21Ala for 24 h did not exhibit a decrease in activatable CaMKII (Fig. 2*B*).

We previously showed that neuronal uptake of fluorescent carboxyfluorescein (Fam)-labeled tat-CN21 and control tat-

CN21Ala (Fam conjugated to the C terminus) were similar in our cortical cultures (12). Using these Fam-labeled peptides, we measured peptide uptake and neuronal death to identify whether fluorescently labeled neurons are preferentially dying in our assay. Using fluorescent microscopy, we observed that ~25% of cells display substantial tat-CN21-Fam or tat-CN21Ala-Fam uptake (supplemental Fig. 2). However, a large proportion of cells exhibit low but still above background levels of fluorescent peptide, suggesting that CaMKII activity may be reduced in more than 25% of cells. It is noteworthy that peptide uptake (~25%) correlates with neuronal death (~25%). The disconnect between maximal cell death (~25%) and the 50% decrease in CaMKII activity could be explained by the observation that not all cells exhibit the same levels of peptide uptake, suggesting that low levels of CaMKII inhibition may not reach a threshold that is required for neurotoxicity. Although the mechanism behind the differential peptide uptake and loss of CaMKII activity is not known, there is a clear correlation with cytotoxicity and CaMKII inhibitor uptake as nearly 80% of cytotoxic cells exhibit tat-CN21-Fam co-localization (supplemental Fig. 2).

CaMKII Inhibition Induces Apoptosis—The time dependence of CaMKII inhibition (>4 h) leading to toxicity is consistent with apoptosis. To test if neurons were undergoing apoptosis in response to prolonged CaMKII inhibition, cultures were co-treated with tat-CN21, and the protein translation inhibitor cycloheximide. Co-application of 0.5 mg/ml cycloheximide blocked tat-CN21-induced neurotoxicity (Fig. 3A). Similarly, co-treatment of tat-AIP and cycloheximide abolished the tat-AIP-induced toxicity (supplemental Fig. 3). In further support of apoptosis, there was a significant increase in TUNEL staining of cultures treated with tat-CN21 for 24 h compared with control and cultures co-treated with 0.5 mg/ml cycloheximide (Fig. 3B). To confirm that the apoptosis occurred within cells that took up the CaMKII inhibitors, we next examined levels of activated caspase-3, a neuronal marker for apoptosis. Overnight application of tat-CN21-Fam was used to identify neuron uptake of the CaMKII inhibitor. Activated caspase-3 labeling was limited to cells that contained tat-CN21-Fam (Fig. 3C). Not all neurons that were tat-CN21-Fam-positive displayed caspase-3 activation. However, nearly all of the neurons that contained tat-CN21-Fam had pyknotic and fragmented nuclei, indicating that the neurons were compromised (Fig. 3C). Thus, although some necrotic cell death may not be ruled out, CaMKII inhibition does lead to apoptosis.

Calcium Dysregulation with CaMKII Inhibition—One prominent mechanism underlying neurodegeneration is dysregulated calcium signaling (31). Cultured hippocampal neurons (DIV 14) were loaded with Fura-2FF-AM, and intracellular calcium levels were measured using ratiometric fluorescent imaging. Although tat-CN21Ala or tat did not alter intracellular calcium levels, tat-CN21 led to a gradual rise in intracellular calcium (Fig. 4, B–D), suggesting that CaMKII inhibition leads to a slow, tonic increase in intracellular calcium. This calcium dysregulation is also observed in cortical neurons loaded with Fluo-4-AM. Using this high affinity calcium indicator, we observed significantly elevated intracellular calcium levels occurring within 10 min of exposure to tat-CN21 application
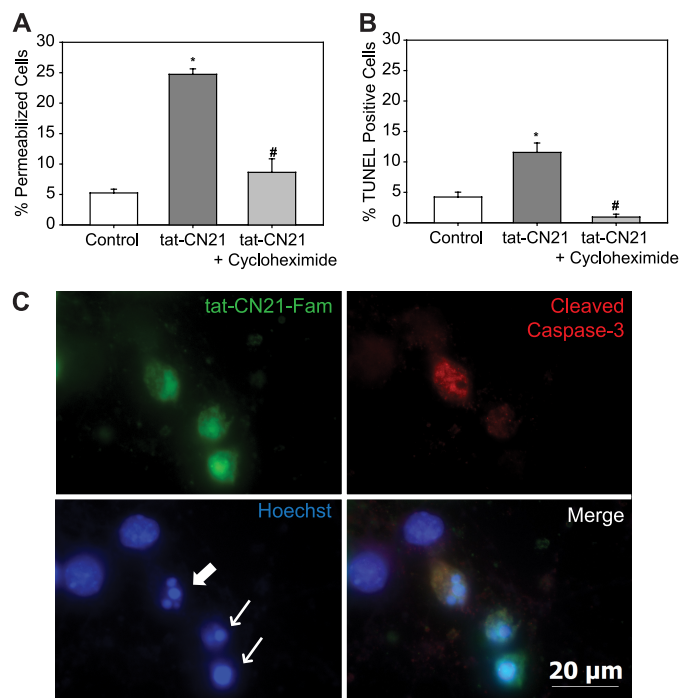

FIGURE 3. **Neuronal apoptosis with CaMKII inhibition.** Neuronal death (mean ± S.E., n = 5–10) following treatment with tat-CN21 with or without 0.5 mg/ml cycloheximide as measured by ethidium homodimer membrane permeability dye (A) or TUNEL staining (B). *, $p < 0.05$ compared with control; #, $p < 0.05$ compared with tat-CN21 alone (one-way ANOVA, post hoc Dunnett's test). C, representative image of a field of neurons treated with 10 μM tat-CN21-Fam for 24 h (*top left*) immunostained for cleaved caspase-3 (*top right*), nuclear marker Hoechst (*bottom left*), and a merge of all three channels (*bottom right*). Arrows indicate fragmented or pyknotic nuclei.

(Fig. 4, E and F). Again, no changes in intracellular calcium were observed with tatCN21-Ala (Fig. 4E). Similar to tat-CN21, 10 μM tat-AIP (data not shown) and 10 μM myristoylated AIP (Fig. 4F) induced a significant increase in intracellular calcium concentration. In contrast, inhibition of the CaMKK pathway (CaMKI and CaMKIV (32, 33)), using STO-609, does not induce calcium dysregulation (Fig. 4F). Thus, acute CaMKII inhibition leads a slow increase in intracellular calcium levels.

Low extracellular calcium largely prevented the tat-CN21-induced calcium influx (Fig. 4F), indicating that calcium influx is likely derived from extracellular sources. L-type voltage-gated calcium channels do not appear to contribute to this process because pretreatment with 10 μM nimodipine had no effect on tat-CN21-induced calcium dysregulation (Fig. 4F). However, synaptic transmission may contribute to the increase in intracellular calcium, as 1 μM N-type calcium channel blocker ω-conotoxin abolished calcium dysregulation prior to tat-CN21 treatment. Because N-type calcium channels play a prominent role in synaptic activity, we tested if neuronal activity was essential for this process by inhibiting AMPA receptors. Indeed, inhibition of AMPA receptors, using 10 μM 6-cyano-7-nitroquinoxaline-2,3-dione blocked calcium dysregulation following CaMKII inhibition. In further support for neuronal activity being essential for the tonic increase in intracellular calcium observed with CaMKII inhibition, inhibition of voltage-gated sodium channels using tetrodotoxin (1 μM) prior to tat-CN21 treatment completely abolished the calcium influx (Fig. 4F). These data are consistent with neuronal activity being
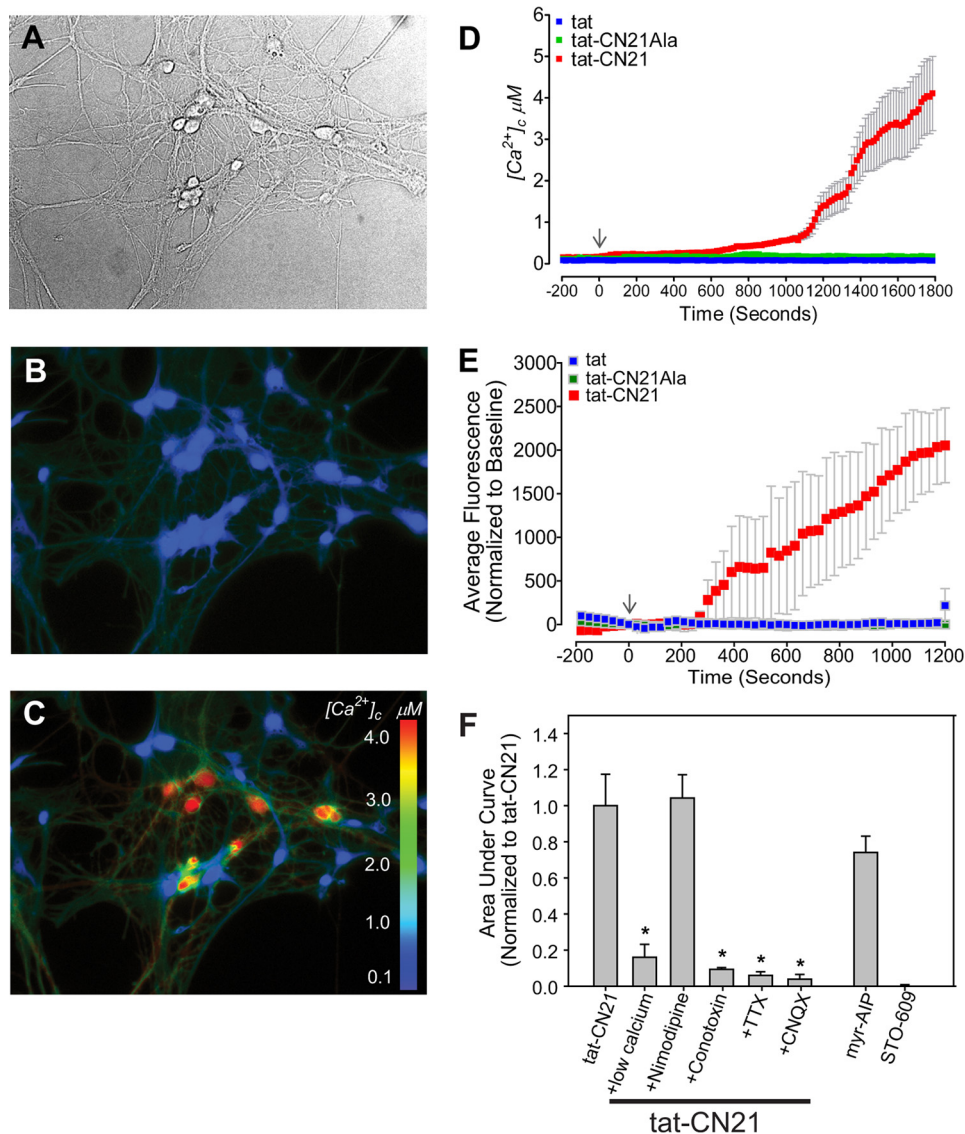
FIGURE 4. **Calcium dysregulation with CaMKII inhibition in hippocampal neurons.** *A,* representative bright field; *B* and *C,* fluorescent images of Fura-2FF-loaded hippocampal neurons. *B,* before treatment; *C,* after treatment with 10 μM tat-CN21. *D,* cytoplasmic calcium levels ([Ca^{2+}]$_c$) (mean ± S.E.) before and after application of 10 μM tat-CN21, tat-CN21Ala, or tat. *E,* neuronal intracellular calcium levels (mean ± S.E.) before (−300 to 0 s) and after (0 to 1200 s) application of 10 μM tat-CN21, tat-CN21Ala, or tat, as measured by Fluo-4 ($n = 4$). *F,* average integral of fluorescent intensity from 0 to 1200 s in *E* (mean ± S.E., $n = 3$–6) with application of CaMKII inhibitors with and without pharmacological blockers of neuronal excitability. The integral was normalized to the calcium influx observed with application of 10 μM tat-CN21. *, $p < 0.05$ compared with tat-CN21 alone (one-way ANOVA, post hoc Dunnett's test).

essential for the calcium influx associated with inhibition of CaMKII.

Enhanced Neuronal Excitability with CaMKII Inhibition—To address the potential for CaMKII inhibition to alter neuronal excitability, we employed whole cell current clamp to measure action potential firing in response to a depolarizing voltage ramp. In these experiments we used a lower peptide concentration (1 μM) because the patch pipette provides direct access to the cytosol. We used inhibitory peptides without the cell-penetrating tat motif to affect only the cell from which we were recording. Each cell served as its own control by determining the number of action potentials generated immediately after establishing whole cell configuration *versus* 10 min later when the peptide inhibitors have had the opportunity to diffuse from the pipette to inhibit CaMKII. Cortical neurons exposed to 1 μM CN21 for 10 min exhibited a 3-fold increase in the number

of action potentials compared with neurons treated with 1 μM inactive peptide CN21Ala (Fig. 5, *A* and *B*). CN21C, another previously established control for CN21 (12, 13), did not result in a significant increase in action potential number compared with base line. Overall, these data support the hypothesis that CaMKII inhibition enhances neuronal excitability.

CaMKII Inhibition Predisposes Neurons to Excitotoxic Insults—Our observed increase in neuronal excitability with a loss of CaMKII activity supports previous reports indicating that genetic αCaMKII knock-out animals are predisposed to epilepsy (34). We hypothesize that this increased excitability not only underlies the observed neurotoxicity but also mechanistically underlies the decreased ability of the neurons to handle excitatory insults. As mentioned, αCaMKII knock-out animals also exhibit greater neuronal damage following middle cerebral artery occlusion than their wild-type littermates (18). Similarly,
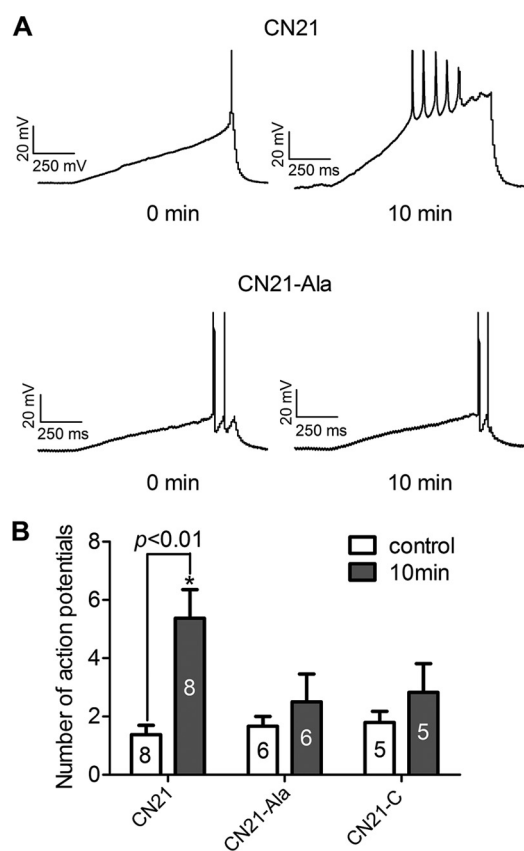
FIGURE 5. **CaMKII inhibition augments neuronal excitability.** *A,* representative traces from cortical neurons at time 0 and 10 min following diffusion of either 1 μM CN21 or 1 μM CN21Ala. Neurons were held at their resting membrane potentials and injected with 1-s depolarizing current ramps to evoke action potentials. *B,* number of action potentials (mean ± S.D.) evoked at time 0 or 10 min after whole cell configuration in the presence of CN21 or control CN21Ala or CN21C. *, $p < 0.01$ between the number of action potentials between time 0 and 10 min (one-way ANOVA, post hoc Bonferroni).

FIGURE 6. **Prolonged CaMKII inhibition sensitizes neurons to excitotoxicity-related insults.** Neuronal death (mean ± S.E., $n = 3–7$) following treatment with various combinations of tat-CN21, NMDA, H_2O_2, or microcystin-LR. All cell death measurements were made 48 h from the start of treatments. Cultures were treated with NMDA, H_2O_2, or microcystin-LR independently or in combination with a 24-h pretreatment of 10 μM tat-CN21. The *clear boxes* highlight the potential levels of cytotoxicity if the average death induced by tat-CN21 treatment alone would be additive. *, $p < 0.05$ compared with control (one-way ANOVA, post hoc Dunnett's test). #, $p < 0.05$ compared with NMDA treatment alone (*t* test). @, $p < 0.05$ compared with H_2O_2 alone (*t* test).

overnight inhibition of CaMKII with tat-CN21 exacerbated cortical cell death following application of exogenous glutamate in an *in vitro* model of excitotoxicity (12). To further explore the role of CaMKII inhibition in sensitizing neurons to excitotoxicity-related insults, we sought to identify whether prolonged CaMKII inhibition predisposed neurons specifically to NMDA-R activation and/or sensitized neurons to the deleterious effect of reactive oxygen species. Thus, 10 μM tat-CN21 was applied to cortical neurons for 24 h. Following overnight inhibition of CaMKII, the neurons were subjected to submaximal levels of 100 μM NMDA, 10 μM glycine or H_2O_2 for 5 min, washed, and 24 h later cell viability assessed. Compared with cultures that were treated with NMDA for 5 min alone, cultures subjected to CaMKII inhibition prior to NMDA-R stimulation exhibited significantly increased neuronal death (15 *versus* 45%) (Fig. 6). Similarly, neurons treated with tat-CN21 also exhibited significantly higher levels of toxicity when treated with H_2O_2, compared with H_2O_2 alone (Fig. 6). Neuronal sensitivity to microcystin-LR, a cell-permeable protein phosphatase 1 and 2A inhibitor, was also assessed as CaMKII activity has been shown to be necessary for microcystin-induced apoptosis (35). Interestingly, prolonged CaMKII inhibition was not synergistic nor additive with microcystin toxicity (Fig. 6), suggesting that CaMKII inhibition via tat-CN21 blocks neurotoxicity
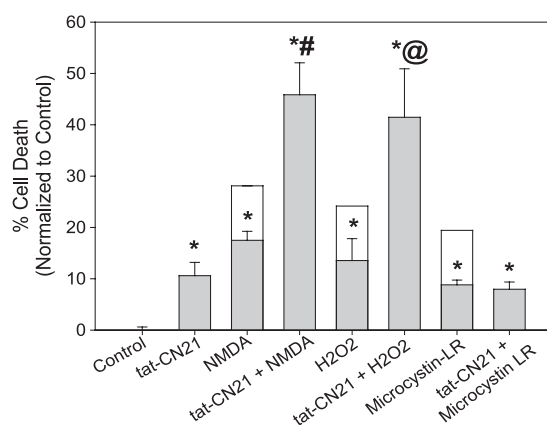
produced by microcystin treatment and that the neuronal death induced by CaMKII inhibition is not obstructed by protein phosphatase inhibitors. Together these data suggest that a prolonged loss of CaMKII sensitizes neurons to reactive oxygen species and NMDA-R-mediated excitotoxicity. Thus, CaMKII inhibition appears toxic to neurons both directly by inducing calcium dysregulation and hyperexcitability and indirectly by predisposing neurons to glutamate excitotoxicity.

Glutamate Dysregulation with CaMKII Inhibition—Because a loss of CaMKII predisposes neurons to glutamate excitotoxicity, we questioned whether CaMKII inhibition itself affected glutamate levels within our cultures. To address this question, cultures were treated with tat-CN21 for varying lengths of time, and glutamate concentration in the media was assessed using a glutamate oxidase assay. There was a significant increase in glutamate concentration in the media as early as 20 min following tat-CN21 application (Fig. 7). Twenty four hours following tat-CN21 application, the concentration of glutamate in the bath solution was 4–5 μM, whereas tat-CN21Ala failed to raise glutamate levels compared with control without treatment (0.5–1 μM). Similarly, HPLC analysis of glutamate concentration in the media also indicated that 24-h application of tat-CN21 resulted in more than a 2-fold elevation in glutamate concentration compared with inactive tat-CN21Ala (supplemental Fig. 4).

To determine whether this slight elevation in glutamate is important for calcium dysregulation and cell death, we sought to attenuate the glutamate rise enzymatically to dissociate CaMKII inhibition with the increased extracellular glutamate. Glutamate pyruvate transaminase (GPT), in the presence of pyruvate, catalyzes the conversion of glutamate to α-ketoglutarate and alanine (35). Thus, we added 0.25 mg/ml GPT and 2 mM pyruvate in combination with the CaMKII inhibitory peptide tat-CN21 to the cortical neurons and measured extracellular glutamate levels using the oxidase assay. Twenty four-hour application of tat-CN21 resulted in a significant increase in glu-
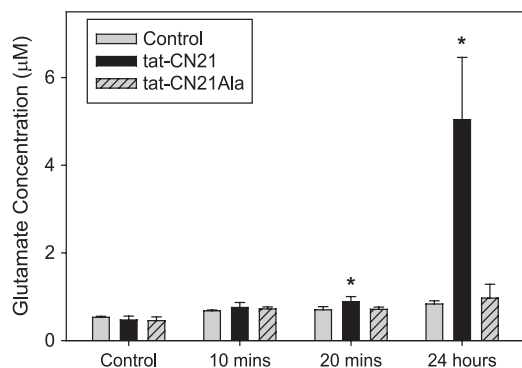
FIGURE 7. **CaMKII inhibition results in increased glutamate in conditioned neuronal media.** Glutamate concentration (mean ± S.D., $n = 3–6$) in neuronal media following incubation with 10 μM tat-CN21 or tat-CN21Ala for varying lengths of time, as measured by a glutamate oxidase assay. *, $p < 0.05$ compared with vehicle control (DMSO) (one-way ANOVA, post hoc Dunnett's test).

tamate in the media of the cultured cortical neurons (Fig. 8*A*). Co-application of GPT and pyruvate with tat-CN21 brought glutamate levels back to control. When pyruvate was omitted from the treatment, a significant increase in glutamate concentration was seen with tat-CN21 (Fig. 8*A*). Furthermore, when GPT was boiled prior to application, GPT and pyruvate failed to bring tat-CN21-induced glutamate release back to control levels (Fig. 8*A*).

Having successfully buffered the prolonged rise in extracellular glutamate when CaMKII was inhibited, we measured acute changes in intracellular calcium concentrations with Fluo-4-AM when GPT and pyruvate were present. As before, 10 μM tat-CN21 induced significant dysregulation of intracellular calcium concentrations within minutes of application (Fig. 8*B*). Interestingly, application of GPT and pyruvate prevented tat-CN21-induced calcium influx (Fig. 8*B*). Co-application of tat-CN21 with pyruvate alone did not alter calcium influx with CaMKII inhibition (0.85 ± 0.24, normalized to tat-CN21).

Neuronal viability following CaMKII inhibition was also assessed with extracellular glutamate buffering. Consistent with the glutamate experiments, the tat-CN21-induced neurotoxicity was abolished by co-treatment with GPT and pyruvate (Fig. 8*C*). Cultures treated with GPT/tat-CN21 exhibited a statistical increase in neuronal death, similar to cultures treated with tat-CN21 alone (Fig. 8*C*). Significant neurotoxicity was also observed when cultures were treated with pyruvate and tat-CN21 (19.077 ± 1.876%). Again, both omission of pyruvate and boiling of GPT prior to application resulted in a failure in preventing tat-CN21-induced neurotoxicity (Fig. 8*C*). Together, these data indicate that enzymatically degrading the glutamate released after CaMKII inhibition prevents calcium dysregulation and neuronal death.

We next examined if calcium entering through glutamate receptors, specifically the NMDA receptor, contributes to the observed calcium influx. Application of 20 μM MK-801 reduced tat-CN21-induced calcium influx by ~80% (Fig. 9*A*). As mentioned earlier, the calcium influx induced by CaMKII inhibition was also blocked by pharmacological antagonism of synaptic activity (via blockade of voltage-gated sodium channels, AMPA
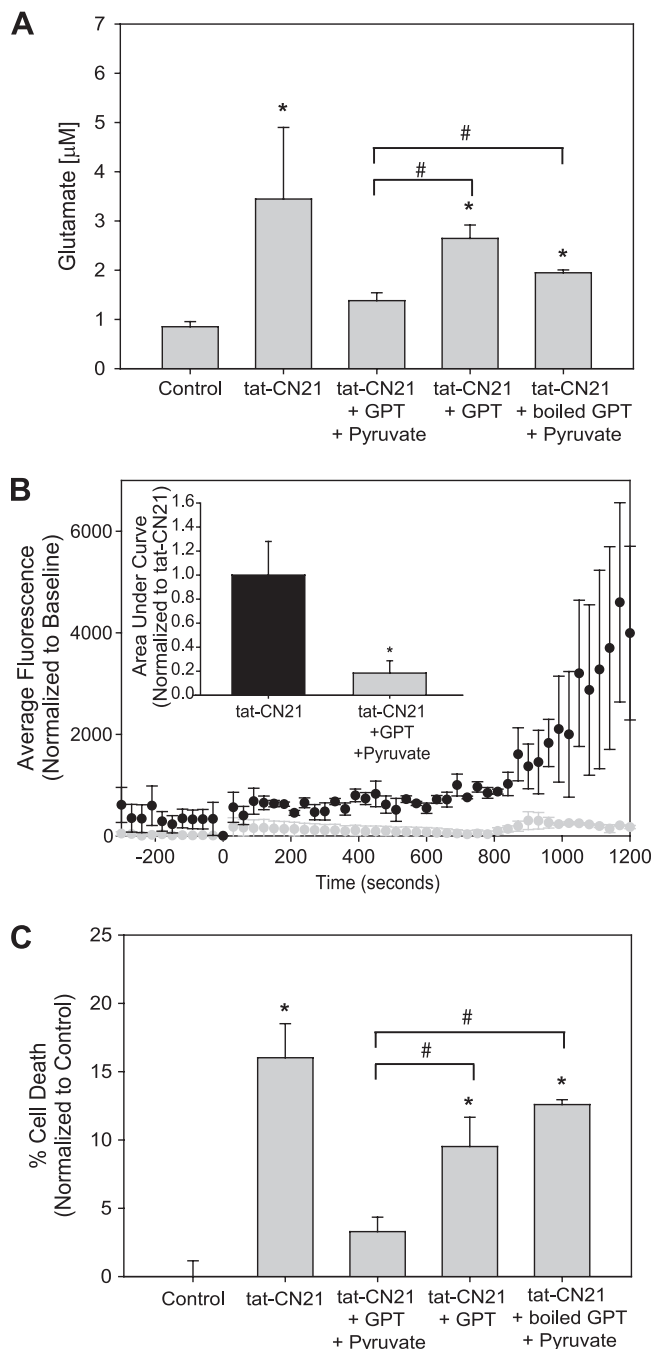
FIGURE 8. **Enzymatic catalysis of glutamate prevents acute and prolonged effects of CaMKII inhibition.** *A*, glutamate concentration (mean ± S.D., $n = 4–8$) in neuronal media following incubation with 10 μM tat-CN21 for 24 h with and without co-application of GPT/pyruvate, GPT alone, or boiled GPT/pyruvate. *, $p < 0.05$ compared with control; #, $p < 0.05$ compared with tat-CN21/GPT/pyruvate treatment (one-way ANOVA, post hoc Dunnett's test). *B*, neuronal intracellular calcium levels (mean ± S.E., $n = 3$) following application of tat-CN21 in the presence or absence of GPT/pyruvate. *Bar graph inset* indicates the average integral from 0 to 1200 s (mean ± S.E., $n = 3$) for these treatment groups. *C*, neuronal death (mean ± S.E., $n = 3–6$) after 24 h of treatment with 10 μM tat-CN21 alone or co-application with GPT/pyruvate, GPT alone, or boiled GPT/pyruvate. *, $p < 0.05$ compared with control; #, $p < 0.05$ compared with tat-CN21/GPT/pyruvate treatment (one-way ANOVA, post hoc Dunnett's test).

receptors, and voltage-gated calcium channels). To determine the contribution of synaptic NMDA receptors in this calcium dysregulation, cortical neurons were treated with bicuculline to
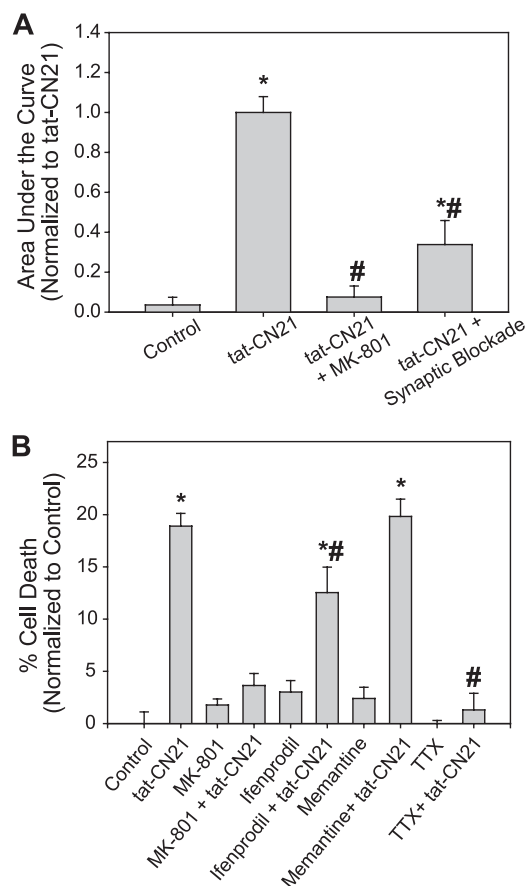
A

B

FIGURE 9. **Pharmacological antagonism of the NMDA receptor prevents acute and prolonged effects of CaMKII inhibition.** *A,* average integral of fluorescent intensity from 0 to 1200 s (mean $\pm$ S.E., $n = 3$–6) reflecting calcium influx in control neurons, or neurons subjected to treatment with tat-CN21 alone or in combination with 20 μM MK-801 or in combination with a prior synaptic NMDA-R blockade. To block synaptic NMDA-Rs before tat-CN21 treatment, 10 μM bicuculline was applied to allow synaptic activity, followed by the addition of 20 μM MK-801 to inhibit the synaptic NMDA-Rs opened as a result of this synaptic activity. *, $p < 0.05$ compared with control; #, $p < 0.05$ compared with tat-CN21 (one-way ANOVA, post hoc Dunnett's test). *B,* neuronal death (mean $\pm$ S.E., $n = 4$–24) after 24 h of treatment with 10 μM tat-CN21 alone or in the presence of 20 μM MK-801, 10 μM ifenprodil, 1 μM memantine, or 200 nM tetrodotoxin (*TTX*). *, $p < 0.05$ compared with control; #, $p < 0.05$ compared with tat-CN21 (one-way ANOVA, post hoc Dunnett's test).

induce synaptic activity by inhibiting GABAergic signaling as described previously (36, 37). Rapid increases in cytoplasmic calcium were observed with bicuculline treatment. MK-801 was added immediately following exposure to bicuculline to block the open NMDA-Rs (supplemental Fig. 5) (38). The CaMKII inhibitor, tat-CN21, was then applied, and subsequent changes in intracellular calcium concentration were monitored. Interestingly, this blockade of synaptic NMDA-Rs significantly blunted tat-CN21-induced calcium influx (Fig. 9A). However, this treatment did not maintain levels of intracellular calcium to those observed in control, indicating that although much of the calcium influx observed with CaMKII inhibition was via the synaptic NMDA receptors, calcium entering through extrasynaptic NMDA-Rs may also contribute to this process.

Because antagonism of the NMDA receptor successfully blunted the acute increase in calcium influx, we hypothesized
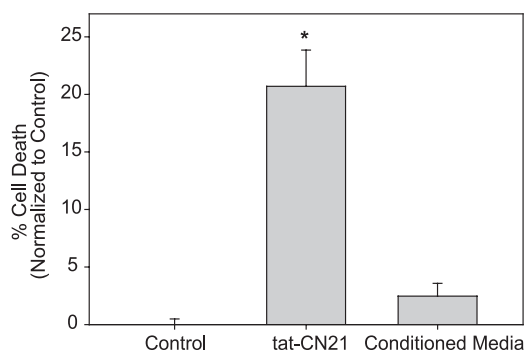

FIGURE 10. **Conditioned media from neurons treated with CaMKII inhibitors does not induce neurotoxicity.** Neuronal death (mean $\pm$ S.E., $n = 3$–9) in neurons treated with 10 μM tat-CN21 for 24 h or naive neurons treated for 24 h with media removed from tat-CN21-treated neurons. *, $p < 0.05$ compared with control (one-way ANOVA, post hoc Dunnett's test).

that MK-801 would also reduce the neurotoxicity induced by CaMKII inhibition. Compared with cultures treated with tat-CN21 alone, neurotoxicity was reduced nearly 80% when tat-CN21 was co-applied with 20 μM MK-801 (Fig. 9B). We next attempted to block extrasynaptic NMDA-Rs to determine the influence of extrasynaptic *versus* synaptic NMDA-Rs to the neurotoxicity induced by CaMKII inhibition. Low levels of ifenprodil and memantine have been shown to be preferential antagonists to the NR2B-containing extrasynaptic NMDA-Rs (39, 40). There was still a significant increase in the observed neurotoxicity when tat-CN21 was co-applied with 10 μM ifenprodil or 1 μM memantine, with neither drug affecting viability alone (Fig. 9B). However, ifenprodil does reduce the levels of toxicity below that observed with tat-CN21 alone (Fig. 9B), suggesting that extrasynaptic NMDA-Rs may play a partial role in the toxicity associated with the loss of CaMKII signaling. Increasing the dose of memantine to 10 μM, a level that inhibits not only extrasynaptic NMDA-Rs but also partially inhibits synaptic NMDA-Rs, does significantly reduce neuronal death (13.6 $\pm$ 4.6%). When cultures were treated with low levels of tetrodotoxin (200 nM) to block action potential induced synaptic activity, tat-CN21-induced toxicity was brought back to base line (Fig. 9B). Thus, although extrasynaptic NMDA-Rs cannot be ruled out, it is quite convincing that synaptic activity is necessary for both the calcium dysregulation and neurotoxicity associated with a loss of CaMKII signaling (39, 40). In total, these data suggest that CaMKII inhibition induces a slow tonic excitotoxic event via calcium dysregulation, enhanced neuronal excitability, and augmented extracellular glutamate levels.

Finally, to determine whether the accumulation of glutamate in the bath solution was solely responsible for this neurotoxicity, cortical neurons were treated for 24 h with 10 μM tat-CN21. The conditioned media were then removed from these cultures and directly applied to naive cortical neurons. Neurons treated with the conditioned media did not display a significant difference in viability compared with nontreated control cultures (Fig. 10). We also did not observe significant neuronal death when 4 μM glutamate was applied to our cortical cultures for 24 h (6.9 $\pm$ 3.1% *versus* control 5.8 $\pm$ 2.2%), suggesting that this glutamate concentration in the media was not sufficient to induce neuronal death in the absence of CaMKII inhibition. Thus, although the increased extracellular glutamate resulting

from CaMKII inhibition is necessary for the observed neurotoxicity (Figs. 8 and 9), it is not sufficient to produce the toxicity itself. Together, these data indicate that the combination of elevated glutamate with the loss of CaMKII activity induces toxicity. Thus, the mechanism underlying the neurotoxicity with CaMKII inhibition was the decreased ability of neurons to tolerate glutamate stimulation, *including* the stimulation resulting from the low levels of glutamate associated with the neuronal hyperactivity directly resulting from CaMKII inhibition.

DISCUSSION

Prolonged CaMKII inhibition using both small molecule (KN-93) and peptide (tat-AIP, myristoylated AIP, and tat-CN21) inhibitors is toxic to cultured neurons in the presence and absence of astrocytes. Although an acute 1-h exposure is not toxic, all of these inhibitors produced neuronal death after 24 h. We elected to use pharmacological approaches over genetic knockdown of CaMKII to better mimic the time course of CaMKII inactivation associated with ischemic brain trauma and other diseases associated with aberrant neuronal activity. Pharmacological inhibitors afford the opportunity to determine acute changes in neuronal activity and calcium homeostasis with CaMKII inhibition. In addition, the CaMKII inhibitors used are not thought to display any isoform specificity, avoiding potential complications associated with isoform compensation associated with genetic knockdown. Multiple pharmacological inhibitors (small molecule and peptide) employing different methodologies for cell uptake (cell-permeable small molecule *versus* tat and myristoylated peptide import strategies) were used to limit the possibility of off-target effects confounding our conclusions.

The concentration of tat-CN21 (10 μM) used throughout this study is similar to previous studies using this CaMKII inhibitor to explore neurite extension (27) and neuroprotection to a glutamate insult (12, 13). Although these values are ~100-fold over the IC$_{50}$ value for CN21 *in vitro* (12, 27), cell uptake and bioavailability can be limiting for intracellular peptide inhibitors (30), making the peptide concentrations used in this and other studies reasonable pharmacological concentrations. Finally, previously established inactive controls for KN-93 (KN-92) (27) and tat-CN21 (tat-CN21Ala) (12) did not induce neuronal death at the concentration of the active inhibitors that clearly produced toxicity, suggesting that the neuronal toxicity observed is due to CaMKII inactivation.

Prolonged CaMKII inhibition is consistent with features of both necrotic and apoptotic cell death. Apoptotic cell death is supported by the following observations. 1) Application of the inhibitors required an incubation period of >8 h to induce toxicity. 2) Inhibitor application led to an increase in TUNEL staining. 3) Co-localization between neurons that take up fluorescent tat-CN21 and cleaved caspase-3 was observed. 4) Cell death was prevented by the protein translation inhibitor, cycloheximide. The pro-apoptotic Bcl-2-associated death promoter (BAD) protein is inactivated by CaMKII phosphorylation. Thus, it is possible that the prolonged inhibition of CaMKII activity disinhibits the BAD cascade, leading to apoptosis (41). A population of neurons containing the CaMKII inhibitor did

not exhibit caspase-3 staining, yet these neurons consistently exhibited morphological changes in the nucleus (condensation and fragmentation). It is unclear whether these neurons represent a continuum between necrosis and apoptosis or whether this could be specifically related to apoptosis with secondary necrosis (42).

CaMKII inhibition results in a slow sustained increase in intracellular calcium levels that is accompanied by elevated glutamate and enhanced neuronal excitability. Calcium dysregulation occurs within 10–20 min of exposure to tat-CN21; a time course that correlates with maximal fluorescent uptake of tat-based peptides in our cortical cultures (12). Although L-type voltage-gated calcium channels do not appear to contribute to calcium dysregulation following CaMKII inhibition, ion channels regulating neuronal activity (voltage-gated sodium channels and N-type voltage-gated calcium channel) are critical for this process. Consistent with synaptic coupling required for calcium dysregulation, we observed that functional glutamate receptors (AMPA and NMDA subtypes) and elevated glutamate are necessary for this process. Although synaptic NMDA-Rs appeared to largely dictate calcium dysregulation and neuronal toxicity to CaMKII inhibition, we cannot rule out a contribution played by extrasynaptic NMDA-Rs in these processes. The involvement of both synaptic and extrasynaptic NMDA-Rs in calcium dysregulation and toxicity is reasonable considering that elevated levels of glutamate appear to accumulate in the media over time, with enhanced extracellular glutamate levels observed as early as 20 min following exposure to CaMKII inhibitors. Thus, although increased synaptic transmission may be necessary, it is possible that once glutamate accumulates in the milieu, it can also activate receptors outside of the synaptic cleft. Interestingly, exposure to elevated glutamate using conditioned media or exogenous glutamate is not toxic in the absence of CaMKII inhibition, suggesting that glutamate by itself is not sufficient for neurotoxicity in the absence of CaMKII inhibition. However, the elevated extracellular glutamate in conjunction with CaMKII inhibition appears to be essential to both calcium dysregulation and neurotoxicity, as enzymatic buffering of extracellular glutamate or pharmacological inhibition of the AMPA or NMDA receptors prevents calcium dysregulation. The fact that media exchange after 4 h prevents neuronal toxicity to CaMKII inhibition is consistent with these observations, further supporting an important functional and temporal association between CaMKII inhibition and neuronal activity in this form of neurotoxicity.

Although our data do not rule out the possibility that elevated extracellular glutamate is produced by cell lysis, the observation that an increase in the number of action potentials induced by a depolarizing current following CaMKII inhibition by localized delivery of the CN21 inhibitor to individual cortical neurons supports the hypothesis that CaMKII inhibition directly enhances neuronal excitability. This acute response in neuronal excitability to CaMKII inhibition is novel. However, genetic knockdown of αCaMKII in mice (34) or neuronal cultures by siRNA (43) support these findings. Thus, results from experiments examining the effect of CaMKII inhibition via pharmacological (this study) or genetic approaches (34, 43)

support the hypothesis that CaMKII is a major regulator of neuronal excitability.

Our experiments favor a model whereby the sustained inhibition of CaMKII activity instigated a vicious cycle of sustained increases in intracellular calcium because of sustained glutamate release. In essence, CaMKII inhibition initiates an excitotoxic cycle by increasing neuronal excitability that subsequently supports enhanced glutamate levels in the media; a feed-forward cycle can be broken by preventing neuronal activity, blocking calcium dysregulation, or by removing extracellular glutamate. These data suggest that CaMKII may be viewed to function in neurons as a brake for glutamate excitation and/or as a master regulator of neuronal excitability and calcium homeostasis. Finally, the observed results do not appear to be limited to highly purified cortical cultures, as co-cultures of cortical neurons with astrocytes also display neuronal death following CaMKII inhibition. We cannot rule out the potential of glial function or viability being altered following CaMKII inhibition in mixed cultures, as glial cells also express CaMKII (44), and thus on-going experiments will need to examine consequences of CaMKII inhibition in astrocyte function and survival.

How could CaMKII inhibition impact calcium-induced neuronal death during ischemia and other excitotoxic stimuli? CaMKII has been shown to inactivate in the core of an ischemic insult as well as in the surrounding penumbral tissue *in vivo* (8); these phenomena are also observed following aberrant neuronal activity in epilepsy (45). The mechanism of CaMKII inactivation in these diseases is not well understood, but it is known that CaMKII proteolysis is preceded by post-translational modifications (46), including a soluble to particulate transition consistent with CaMKII aggregation following ischemia (7, 8, 47). Inactivation associated with aggregation is consistent with CaMKII self-association, which is a form of catalytic aggregation that requires calcium/CaM activation and is maximized under ischemic conditions (*i.e.* reduced energy) (48, 49). In this study, we have attempted to mimic one consequence of CaMKII self-association via pharmacological inhibition of enzymatic activity. Similar to *in vivo* studies characterizing functional changes in CaMKII associated with aberrant neuronal activity, we have observed a sustained loss of activatable CaMKII with long term tat-CN21 exposure in cultured cortical neurons. This sustained inactivation and the transition of αCaMKII from the soluble to particulate fractions have been previously shown to also accompany excitotoxic glutamate-glycine insults in neuronal cultures (12, 49). An intriguing hypothesis is that the neuroprotection produced by acute exposure to CaMKII inhibitors may be limiting neurotoxicity to excitotoxic glutamate/glycine challenges by paradoxically preventing excitotoxicity-induced CaMKII inactivation-aggregation.

Independent of this speculation, these results indicate that sustained inactivation of CaMKII leads to neuronal cell death through engagement of apoptotic/necrotic pathways induced by calcium dysregulation and hyperexcitability, which contributes to the decreased capacity of neurons to cope with excitatory insults. These data may provide further mechanistic insight into the increased infarct size observed within αCaMKII knock-out animals (18) and, moreover, to the phenomenon of expanding neuronal damage in the ischemic penumbra. Peri-infarct depolarizations have been shown to underlie the progression of neuronal damage from the core throughout the penumbra (50–52). Interestingly, these depolarizations have been shown to be calcium-dependent and are significantly reduced by NMDA receptor antagonism (51). These findings are consistent with the functional consequences of CaMKII inactivation highlighted in this study. Thus, our working hypothesis is that the extent of neuronal damage in the penumbral region is governed by the loss of CaMKII, which increases neuronal activity and heightens susceptibility to excitotoxicity-related insults, such as glutamate and reactive oxygen species activity.

REFERENCES

1. Coultrap, S. J., Vest, R. S., Ashpole, N. M., Hudmon, A., and Bayer, K. U. (2011) CaMKII in cerebral ischemia. *Acta Pharmacol. Sin.* **32,** 861–872
2. Hudmon, A., and Schulman, H. (2002) Neuronal Ca^{2+}/calmodulin-dependent protein kinase II. The role of structure and autoregulation in cellular function. *Annu. Rev. Biochem.* **71,** 473–510
3. Colbran, R. J. (2004) Targeting of calcium/calmodulin-dependent protein kinase II. *Biochem. J.* **378,** 1–16
4. Perlin, J. B., Churn, S. B., Lothman, E. W., and DeLorenzo, R. J. (1992) Loss of type II calcium/calmodulin-dependent kinase activity correlates with stages of development of electrographic seizures in status epilepticus in rat. *Epilepsy Res.* **11,** 111–118
5. Zalewska, T., and Domanska-Janik, K. (1996) Brain ischemia transiently activates Ca^{2+}/calmodulin-independent protein kinase II. *Neuroreport* **7,** 637–641
6. Churn, S. B., Limbrick, D., Sombati, S., and DeLorenzo, R. J. (1995) Excitotoxic activation of the NMDA receptor results in inhibition of calcium/calmodulin kinase II activity in cultured hippocampal neurons. *J. Neurosci.* **15,** 3200–3214
7. Aronowski, J., Grotta, J. C., and Waxham, M. N. (1992) Ischemia-induced translocation of Ca^{2+}/calmodulin-dependent protein kinase II. Potential role in neuronal damage. *J. Neurochem.* **58,** 1743–1753
8. Hanson, S. K., Grotta, J. C., Waxham, M. N., Aronowski, J., and Ostrow, P. (1994) Calcium/calmodulin-dependent protein kinase II activity in focal ischemia with reperfusion in rats. *Stroke* **25,** 466–473
9. Westgate, S. A., Brown, J., Aronowski, J., and Waxham, M. N. (1994) Activity of Ca^{2+}/calmodulin-dependent protein kinase II following ischemia. A comparison between CA1 and dentate gyrus in a hippocampal slice model. *J. Neurochem.* **63,** 2217–2224
10. Folkerts, M. M., Parks, E. A., Dedman, J. R., Kaetzel, M. A., Lyeth, B. G., and Berman, R. F. (2007) Phosphorylation of calcium calmodulin-dependent protein kinase II following lateral fluid percussion brain injury in rats. *J. Neurotrauma* **24,** 638–650
11. Schwarzbach, E., Bonislawski, D. P., Xiong, G., and Cohen, A. S. (2006) Mechanisms underlying the inability to induce area CA1 LTP in the mouse after traumatic brain injury. *Hippocampus* **16,** 541–550
12. Ashpole, N. M., and Hudmon, A. (2011) Excitotoxic neuroprotection and vulnerability with CaMKII inhibition. *Mol. Cell. Neurosci.* **46,** 720–730
13. Vest, R. S., O'Leary, H., Coultrap, S. J., Kindy, M. S., and Bayer, K. U. (2010) Effective post-insult neuroprotection by a novel Ca^{2+}/calmodulin-dependent protein kinase II (CaMKII) inhibitor. *J. Biol. Chem.* **285,** 20675–20682
14. Hajimohammadreza, I., Probert, A. W., Coughenour, L. L., Borosky, S. A., Marcoux, F. W., Boxer, P. A., and Wang, K. K. (1995) A specific inhibitor of calcium/calmodulin-dependent protein kinase-II provides neuroprotection against NMDA- and hypoxia/hypoglycemia-induced cell death. *J. Neurosci.* **15,** 4093–4101

15. Laabich, A., and Cooper, N. G. (2000) Neuroprotective effect of AIP on *N*-methyl-D-aspartate-induced cell death in retinal neurons. *Brain Res. Mol. Brain Res.* **85,** 32–40

16. Fan, W., Agarwal, N., and Cooper, N. G. (2006) The role of CaMKII in BDNF-mediated neuroprotection of retinal ganglion cells (RGC-5). *Brain Res.* **1067,** 48–57

17. Goebel, D. J. (2009) Selective blockade of CaMKII-α inhibits NMDA-induced caspase-3-dependent cell death but does not arrest PARP-1 activation or loss of plasma membrane selectivity in rat retinal neurons. *Brain Res.* **1256,** 190–204

18. Waxham, M. N., Grotta, J. C., Silva, A. J., Strong, R., and Aronowski, J. (1996) Ischemia-induced neuronal damage: a role for calcium/calmodulin-dependent protein kinase II. *J. Cereb. Blood Flow Metab.* **16,** 1–6

19. Dubinsky, J. M. (1993) Intracellular calcium levels during the period of delayed excitotoxicity. *J. Neurosci.* **13,** 623–631

20. Brustovetsky, T., Li, V., and Brustovetsky, N. (2009) Stimulation of glutamate receptors in cultured hippocampal neurons causes Ca^{2+}-dependent mitochondrial contraction. *Cell Calcium* **46,** 18–29

21. Kolb, S. J., Hudmon, A., and Waxham, M. N. (1995) Ca^{2+}/calmodulin kinase II translocates in a hippocampal slice model of ischemia. *J. Neurochem.* **64,** 2147–2156

22. Brustovetsky, T., Brittain, M. K., Sheets, P. L., Cummins, T. R., Pinelis, V., and Brustovetsky, N. (2011) KB-R7943, an inhibitor of the reverse Na^+/Ca^{2+} exchanger, blocks *N*-methyl-D-aspartate receptor and inhibits mitochondrial complex I. *Br. J. Pharmacol.* **162,** 255–270

23. Zhang, Y. H., Chi, X. X., and Nicol, G. D. (2008) Brain-derived neurotrophic factor enhances the excitability of rat sensory neurons through activation of the p75 neurotrophin receptor and the sphingomyelin pathway. *J. Physiol.* **586,** 3113–3127

24. Wang, Y., Nicol, G. D., Clapp, D. W., and Hingtgen, C. M. (2005) Sensory neurons from Nf1 haploinsufficient mice exhibit increased excitability. *J. Neurophysiol.* **94,** 3670–3676

25. Donzanti, B. A., and Yamamoto, B. K. (1988) An improved and rapid HPLC-EC method for the isocratic separation of amino acid neurotransmitters from brain tissue and microdialysis perfusates. *Life Sci.* **43,** 913–922

26. Chang, B. H., Mukherji, S., and Soderling, T. R. (1998) Characterization of a calmodulin kinase II inhibitor protein in brain. *Proc. Natl. Acad. Sci. U.S.A.* **95,** 10890–10895

27. Vest, R. S., Davies, K. D., O'Leary, H., Port, J. D., and Bayer, K. U. (2007) Dual mechanism of a natural CaMKII inhibitor. *Mol. Biol. Cell* **18,** 5024–5033

28. Ishida, A., Kameshita, I., Okuno, S., Kitani, T., and Fujisawa, H. (1995) A novel highly specific and potent inhibitor of calmodulin-dependent protein kinase II. *Biochem. Biophys. Res. Commun.* **212,** 806–812

29. Sumi, M., Kiuchi, K., Ishikawa, T., Ishii, A., Hagiwara, M., Nagatsu, T., and Hidaka, H. (1991) The newly synthesized selective Ca^{2+}/calmodulin-dependent protein kinase II inhibitor KN-93 reduces dopamine contents in PC12h cells. *Biochem. Biophys. Res. Commun.* **181,** 968–975

30. Tünnemann, G., Martin, R. M., Haupt, S., Patsch, C., Edenhofer, F., and Cardoso, M. C. (2006) Cargo-dependent mode of uptake and bioavailability of TAT-containing proteins and peptides in living cells. *FASEB J.* **20,** 1775–1784

31. Orrenius, S., Zhivotovsky, B., and Nicotera, P. (2003) Regulation of cell death. The calcium-apoptosis link. *Nat. Rev. Mol. Cell Biol.* **4,** 552–565

32. Tokumitsu, H., Inuzuka, H., Ishikawa, Y., Ikeda, M., Saji, I., and Kobayashi, R. (2002) STO-609, a specific inhibitor of the Ca^{2+}/calmodulin-dependent protein kinase kinase. *J. Biol. Chem.* **277,** 15813–15818

33. Schmitt, J. M., Guire, E. S., Saneyoshi, T., and Soderling, T. R. (2005) Calmodulin-dependent kinase kinase/calmodulin kinase I activity gates extracellular-regulated kinase-dependent long term potentiation. *J. Neurosci.* **25,** 1281–1290

34. Butler, L. S., Silva, A. J., Abeliovich, A., Watanabe, Y., Tonegawa, S., and McNamara, J. O. (1995) Limbic epilepsy in transgenic mice carrying a Ca^{2+}/calmodulin-dependent kinase II α-subunit mutation. *Proc. Natl. Acad. Sci. U.S.A.* **92,** 6852–6855

35. Beaton, G. H., Curry, D. M., and Veen, M. J. (1957) Alanine-glutamic transaminase activity and protein metabolism. *Arch. Biochem. Biophys.* **70,** 288–290

36. Hardingham, G. E., Fukunaga, Y., and Bading, H. (2002) Extrasynaptic NMDARs oppose synaptic NMDARs by triggering CREB shut-off and cell death pathways. *Nat. Neurosci.* **5,** 405–414

37. Ivanov, A., Pellegrino, C., Rama, S., Dumalska, I., Salyha, Y., Ben-Ari, Y., and Medina, I. (2006) Opposing role of synaptic and extrasynaptic NMDA receptors in regulation of the extracellular signal-regulated kinases (ERK) activity in cultured rat hippocampal neurons. *J. Physiol.* **572,** 789–798

38. Huettner, J. E., and Bean, B. P. (1988) Block of *N*-methyl-D-aspartate-activated current by the anticonvulsant MK-801. Selective binding to open channels. *Proc. Natl. Acad. Sci. U.S.A.* **85,** 1307–1311

39. Thomas, C. G., Miller, A. J., and Westbrook, G. L. (2006) Synaptic and extrasynaptic NMDA receptor NR2 subunits in cultured hippocampal neurons. *J. Neurophysiol.* **95,** 1727–1734

40. Xia, P., Chen, H. S., Zhang, D., and Lipton, S. A. (2010) Memantine preferentially blocks extrasynaptic over synaptic NMDA receptor currents in hippocampal autapses. *J. Neurosci.* **30,** 11246–11250

41. Bok, J., Wang, Q., Huang, J., and Green, S. H. (2007) CaMKII and CaMKIV mediate distinct prosurvival signaling pathways in response to depolarization in neurons. *Mol. Cell. Neurosci.* **36,** 13–26

42. Bonfoco, E., Krainc, D., Ankarcrona, M., Nicotera, P., and Lipton, S. A. (1995) Apoptosis and necrosis. two distinct events induced, respectively, by mild and intense insults with *N*-methyl-D-aspartate or nitric oxide/superoxide in cortical cell cultures. *Proc. Natl. Acad. Sci. U.S.A.* **92,** 7162–7166

43. Carter, D. S., Haider, S. N., Blair, R. E., Deshpande, L. S., Sombati, S., and DeLorenzo, R. J. (2006) Altered calcium/calmodulin kinase II activity changes calcium homeostasis that underlies epileptiform activity in hippocampal neurons in culture. *J. Pharmacol. Exp. Ther.* **319,** 1021–1031

44. Takeuchi, Y., Yamamoto, H., Fukunaga, K., Miyakawa, T., and Miyamoto, E. (2000) Identification of the isoforms of Ca^{2+}/calmodulin-dependent protein kinase II in rat astrocytes and their subcellular localization. *J. Neurochem.* **74,** 2557–2567

45. Yamagata, Y., Imoto, K., and Obata, K. (2006) A mechanism for the inactivation of Ca^{2+}/calmodulin-dependent protein kinase II during prolonged seizure activity and its consequence after the recovery from seizure activity in rats *in vivo*. *Neuroscience* **140,** 981–992

46. Churn, S. B., Taft, W. C., Billingsley, M. S., Sankaran, B., and DeLorenzo, R. J. (1992) Global forebrain ischemia induces a post-translational modification of multifunctional calcium- and calmodulin-dependent kinase II. *J. Neurochem.* **59,** 1221–1232

47. Tao-Cheng, J. H., Vinade, L., Pozzo-Miller, L. D., Reese, T. S., and Dosemeci, A. (2002) Calcium/calmodulin-dependent protein kinase II clusters in adult rat hippocampal slices. *Neuroscience* **115,** 435–440

48. Hudmon, A., Aronowski, J., Kolb, S. J., and Waxham, M. N. (1996) Inactivation and self-association of Ca^{2+}/calmodulin-dependent protein kinase II during autophosphorylation. *J. Biol. Chem.* **271,** 8800–8808

49. Hudmon, A., Lebel, E., Roy, H., Sik, A., Schulman, H., Waxham, M. N., and De Koninck, P. (2005) A mechanism for Ca^{2+}/calmodulin-dependent protein kinase II clustering at synaptic and nonsynaptic sites based on self-association. *J. Neurosci.* **25,** 6971–6983

50. Fujioka, H., Kaneko, H., Suzuki, S. S., and Mabuchi, K. (2004) Hyperexcitability-associated rapid plasticity after a focal cerebral ischemia. *Stroke* **35,** e346–e348

51. Ohta, K., Graf, R., Rosner, G., and Heiss, W. D. (2001) Calcium ion transients in peri-infarct depolarizations may deteriorate ion homeostasis and expand infarction in focal cerebral ischemia in cats. *Stroke* **32,** 535–543

52. Mies, G., Iijima, T., and Hossmann, K. A. (1993) Correlation between peri-infarct DC shifts and ischemic neuronal damage in rat. *Neuroreport* **4,** 709–711